PHYSICAL REVIEW B **82**, 041301(R) (2010)

Exchange constant and domain wall width in (Ga,Mn)(As,P) films with self-organization of magnetic domains

S. Haghgoo,[1,2] M. Cubukcu,[1,2] H. J. von Bardeleben,[1,2] L. Thevenard,[1,2] A. Lemaître,[3] and C. Gourdon[1,2,*]

[1]*Institut des Nanosciences de Paris, CNRS, UMR 7588, 140 rue de Lourmel, Paris F-75015, France*

[2]*INSP, Université Pierre et Marie Curie, UMR 7588, Paris, France*

[3]*Laboratoire de Photonique et Nanostructures, CNRS, UPR 20, Route de Nozay, Marcoussis F-91460, France*

(Received 10 May 2010; published 1 July 2010)

The incorporation of phosphorus into (Ga,Mn)As epilayers allows for the tuning of the magnetic easy axis from in-plane to perpendicular-to-plane without the need for a (Ga,In)As template. For perpendicular easy axis, using magneto-optical imaging a self-organized pattern of up- and down-magnetized domains is observed. Combining Kerr microscopy, magnetometry, and ferromagnetic resonance spectroscopy, the exchange constant and the domain wall width parameter are obtained as a function of temperature. The former quantifies the effective Mn-Mn ferromagnetic interaction. The latter is a key parameter for domain wall dynamics. The comparison with results obtained for (Ga,Mn)As/(Ga,In)As reveals the improved quality of the $(Ga,Mn)As_{1-y}P_y$ layers regarding domain wall pinning, an increase in the domain wall width parameter and of the effective Mn-Mn spin coupling.

DOI: 10.1103/PhysRevB.82.041301 PACS number(s): 75.50.Pp, 75.60.Ch, 75.70.Ak

Diluted ferromagnetic (FM) (III,Mn)V semiconductors are the subject of intensive research in view of potential applications in the field of spintronics.[1,2] Several proposals for magnetization manipulation using either light-induced magnetization switching between different magnetic easy axes[3,4] or magnetic domain wall (DW) motion[5–8] have emerged. (Ga,Mn)As layers and microtracks with perpendicular magnetic anisotropy are well suited for the investigation of DW propagation. In such layers the intrinsic flow regime for field-driven DW propagation was demonstrated.[7]

One of the properties of this versatile FM semiconductor is the strong dependence of its magnetic anisotropy on epitaxial strain.[1,9–11] This dependence results from the carrier-mediated origin of the ferromagnetism. It arises from the competition between the Mn-induced giant Zeeman splitting and the strain-induced splitting of the valence bands. Recently, it was shown that introducing a few percent of phosphorus in substitution of arsenic in (Ga,Mn)As layers grown on GaAs provides an efficient tuning of the epitaxial strain, from compressive to tensile, due to the smaller ionic radius of phosphorus.[12,13] As expected theoretically, the magnetic easy axis switches from in-plane to out-of-plane orientation upon increasing P concentration. This eliminates the need for a highly mismatched (Ga,In)As buffer layer for realizing out-of-plane anisotropy. This buffer layer was shown to introduce a cross-hatch pattern and emerging dislocations which are detrimental to the propagation of magnetic DWs.[10,11] $(Ga,Mn)As_{1-y}P_y$ films grown directly on a GaAs buffer are expected to contain much less defects. In addition to this structural advantage, $(Ga,Mn)As_{1-y}P_y$ films are appealing for two aspects.[14] First, it is expected that the smaller lattice constant of $(Ga,Mn)As_{1-y}P_y$ will hinder Mn incorporation in interstitial sites, where Mn ions act as charge and magnetic moment compensating defects, thereby favoring higher carrier density than in (Ga,Mn)As. Second, it was predicted that the decrease in the lattice constant should also lead to an increase in the Mn-hole exchange integral J_{pd} and hence of the Curie temperature. In turn, this should lead to an increase in the exchange constant A describing the effective exchange interaction between the Mn spins in the framework of the micromagnetic theory. The determination of A yields the DW width parameter defined as $\Delta = \sqrt{A/K_u}$, where K_u is the uniaxial anisotropy constant. Δ is a key parameter for DW dynamics.[15] The Walker velocity, i.e., the theoretical critical velocity at the crossover from the steady to the precessional flow regimes in the one-dimensional model, depends on Δ as $v_W = \gamma \Delta \mu_0 M_s/2$, where γ is the electron gyromagnetic ratio and M_s the magnetization. Furthermore, in both the steady and precessional regimes, the DW mobility is proportional to Δ.

In FM layers with perpendicular easy axis one of the methods for the determination of the exchange constant A is based on domain theory, i.e., micromagnetic theory applied to self-organized magnetic domains.[16–19] Self-organization of up- and down-magnetized domains in a periodic array results from the competition between the DW energy and the magnetic energy arising from long-range interaction between domains. Up to now, although an estimation of A could be obtained from the domain structure and hysteresis cycle in (Ga,Mn)As,[19] a long-range periodic arrangement of magnetic domains in (III,Mn)V FM semiconductors had not yet been obtained.

In this Rapid Communication we report the observation of self-organized magnetic domains in $(Ga,Mn)As_{1-y}P_y$ FM alloys with perpendicular magnetic anisotropy. We determine the exchange constant A and the DW width parameter Δ from the domain period. An effective exchange coupling constant J_{MnMn} between Manganese spins is then obtained as a function of phosphorus concentration.

The samples were grown by molecular beam epitaxy on GaAs(001) substrates. Details can be found in Refs. 10 and 13. For $(Ga,Mn)As_{1-y}P_y$ samples, the Mn (P) concentration was estimated from a reference (Ga,Mn)As [(Ga,As)P] sample, grown under similar conditions, in particular, a similar substrate temperature. However the determination of Mn and P concentrations is made difficult by the presence of an unknown concentration of interstitial Mn and As in antisites. In sample D, with no phosphorus, the (Ga,Mn)As layer was

TABLE I. (Ga,Mn)$As_{1-y}P_y$ and (Ga,Mn)As sample parameters. The lattice mismatch (lm) is defined as $(a_\perp - a_{sub})/a_{sub}$, where $a_\perp(a_{sub})$ is the lattice parameter of the film (substrate) parallel to the growth axis. ϵ_{zz} is the corresponding calculated strain component. M_s, K_u, and Q are the magnetization, uniaxial anisotropy constant, and anisotropy quality factor, respectively, at temperature $T=4$ K. Q slightly increases with temperature.

Sample	A1	A2	A3	B	C	D
x_{total}Mn(%)	10.4	10.4	10.4	8	7	7
[P](%)	11.3	8.8	7	8.5	7	0
lm (ppm)	−6650	−5120	−4260	−6870	−3580	−10700
ϵ_{zz}(%)	−0.3	−0.2	−0.2	−0.3	−0.2	−0.5
T_C(K)	119	113	139	110	80	125
M_s(kA m^{-1})	53.8	50.8	53.5	46.2	39.2	38.5
K_u(J m^{-3})	8005	5300	5420	5530	3140	8150
Q	4.4	3.3	3.0	4.1	3.2	8.7

grown in the traditional manner on a $Ga_{1-z}In_zAs$ buffer layer ($z=0.098$) in order to achieve perpendicular anisotropy.[10] To improve M_s, the Curie temperature T_C, and the carrier concentration the samples were annealed under N_2 atmosphere at 250 °C for 1 h. For all samples the layer thickness is $d=50$ nm.

The magnetic domain structure was investigated using polar magneto-optical Kerr (MOKE) microscopy at variable temperature.[11] The lateral spatial resolution is 0.9 μm. The light wavelength is 600 (670) nm for the [Ga,Mn)AsP and (Ga,Mn)As] samples. The hysteresis cycle was obtained from the average intensity of MOKE images as a function of the applied field. The temperature dependence of the saturation magnetization $M_s(T)$ and the Curie temperature T_C were obtained from magnetometry using a superconductor quantum interference device. The anisotropy constants were determined from ferromagnetic resonance spectroscopy. The spectra were analyzed using the Smit-Beljers equation and the minimization of the free energy for different alignments of the applied magnetic field.[12,20]

Table I summarizes the characteristics of the six samples which were selected in order to compare layers with the same Mn concentration and different P concentrations (A series, C and D), or the same P concentration and different Mn concentrations (A2 and B, A3 and C). Most of the samples show a T_C around 110 K. T_C is not improved significantly in the (Ga,Mn)$As_{1-y}P_y$ samples as compared to sample D (no phosphorus). The concentration of Mn ions participating in the ferromagnetism x_{eff} is determined from the saturation magnetization M_s at $T=4$ K as $x_{eff}=M_s/(N_0 g\mu_B S)$, where N_0 is the density of cation sites in the lattice and μ_B the Bohr magneton and $S=5/2$. For all samples the ratio x_{eff}/x_{total} is ≈ 0.5, revealing the fact that the incorporation of Mn in interstitial sites is not modified by alloying with phosphorus.

The method employed to determine the exchange constant and the DW width parameter is based on domain theory for layers with perpendicular easy axis.[16] Self-organization of up- and down-magnetized domains in a periodic stripe array minimizes the total energy consisting of the Zeeman energy, the surface energy of the DWs and the stray field energy. The stripe period p (in units of d) in the demagnetized state (zero applied field and zero average magnetization) satisfies the following equation:[16]

$$\lambda_c = \frac{p}{\pi^3 Q}\sum_{n=1}^{\infty}\frac{\sin^2\left(\frac{n\pi}{2}\right)\left\{-pQ-2n\pi(1+Q)+pQ\left[\cosh(2\chi)+\sqrt{1+\frac{1}{Q}}\sinh(2\chi)\right]\right\}}{n^3\left[\sqrt{1+\frac{1}{Q}}\cosh(\chi)+\sinh(\chi)\right]^2},$$

where χ is equal to $(n\pi\sqrt{1+1/Q})/p$. $Q=K_u/(\mu_0 M_s^2/2)$ is the anisotropy quality factor shown in Table I. Q is smaller in the P incorporated samples than in sample D due to the smaller K_u and larger M_s. λ_c is Thiele's length defined as $\sigma/\mu_0 M_s^2 d$ with σ the specific DW energy. Knowing p and Q, one determines λ_c and hence σ. Typically, λ_c is found to be on the order of 1. For a Bloch wall σ is equal to $4\sqrt{AK_u}$. Micromagnetic simulations using OOMMF package[21] show that in our samples with $d=50$ nm DWs are not Bloch walls but twisted walls with Néel caps. Using the variational calculations of Ref. 22 for the DW specific energy of twisted walls we obtain the functional dependence of σ on Q and Δ, namely, $\sigma=4f(Q,\Delta)\Delta K_u$ with $f(Q,\Delta)\leq 1$. For each value of σ we obtain the DW width parameter Δ and hence the exchange constant A.

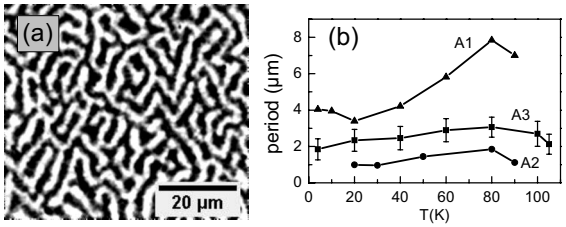

FIG. 1. (a) Self-organized pattern in the demagnetized state for sample A3 at $T=80$ K. (b) Domain period as a function of temperature for samples A1, A2, and A3.

Figure 1(a) shows a typical MOKE image of the self-organized domains with up and down magnetization (white and black) after a demagnetization process in an alternating magnetic field of decreasing amplitude. The remnant field is ≤ 1 G. This image is obtained on sample A3 at $T=80$ K. Figure 1(b) shows the domain period obtained from the MOKE images as a function of the temperature T for samples A1, A2, and A3. Note that at low temperatures, 4 K $\leq T \leq$ 40 K as well as at $T=105$ K the poor contrast in the images for sample A3 leads to less reliable data which will be discussed below. Following the procedure described above, Thiele's length λ_c, the DW specific energy σ, the DW width parameter Δ, and eventually the exchange constant A are obtained. Δ and A are shown in Fig. 2 for sample A3 (filled square symbols) as a function of temperature. Δ is found in the range 7–9 nm and A in the range 0.1–0.4 pJ m^{-1}. The decrease in A with temperature mainly reflects the decrease of the magnetization ($A \propto \lambda_c^2 M^4 / K_u$).

In order to assess the reliability of the Δ and A values at low and high temperature, we determine the upper and lower boundaries for these quantities using the method previously developed for (Ga,Mn)As/GaInAs.[19] The upper boundary for λ_c and consequently for Δ and A is determined from the width of the stripe domains of the minority phase observed close to the saturation field. For sample A3 this upper boundary coincides at all temperatures with the values obtained from the domain period. The lower boundary for λ_c (and hence for Δ and A) is obtained from the comparison of the normalized experimental hysteresis cycle with the calculated magnetization curve $m(h)$, where m is the spatially averaged reduced magnetization $\langle M \rangle / M_s$ and h the reduced applied magnetic field H/M_s. The $m(h)$ curve is obtained from the minimization of the free energy of the periodic stripe array. λ_c is the only free parameter. An example of experimental hysteresis cycle and calculated $m(h)$ curve is given in Fig. 3.

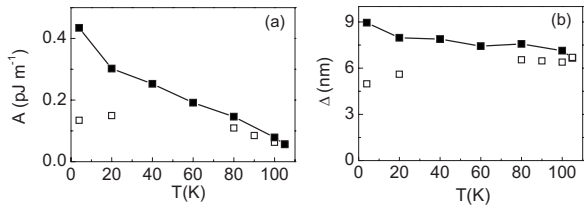

FIG. 2. Exchange constant A (a) and DW width parameter Δ (b) for sample A3. The filled and open symbols represent the values determined from the period of self-organized magnetic domains and from the hysteresis cycle, respectively.

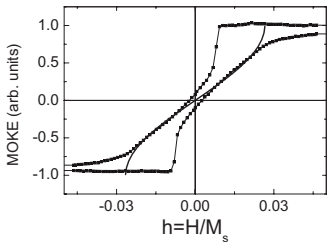

FIG. 3. Experimental hysteresis cycle (symbols) for sample A3 (10.4% Mn, 7% P) at $T=100$ K and calculated $m(h)$ curve for $\lambda_c=0.95$ (solid line).

The $m(h)$ curve which is tangent to the experimental hysteresis cycle provides the lower boundary for λ_c and hence for Δ and A. The values obtained by this method are shown by open symbols in Fig. 2. At high temperature (90–100 K) the lower boundary values coincide with the values determined from the domain period. To summarize, between 4 K and 40 K the DW width parameter and exchange constant are comprised between the values shown by the closed and open symbols of Fig. 2, respectively. Above 40 K Δ and A are reliably obtained from the domain period (filled symbols). Similar results are obtained for samples A1 and A2 where the self-organized domain pattern can be achieved. For samples B and C DW pinning by defects prevents the self-organization of domains in regular patterns. Therefore only the lower and upper boundaries of Δ and A can be obtained, using the method recalled above. For sample C the upper boundary values could not be obtained below 30 K since the stripe domains were not observed. For sample D [(Ga,Mn)As on a (Ga,In)As template] the DW width and exchange constant were obtained from the analysis of the field-driven DW dynamics[7] in excellent agreement with the estimation from the stripe domain width and the hysteresis cycle.[19]

A direct comparison of the exchange constant A between the A, B, C, and D samples is not relevant because of their different effective Mn concentrations. Therefore, using Kittel's relation between the first-neighbor spin-spin interaction constant and the exchange constant A of the micromagnetic theory,[23] we obtain an effective interaction constant between manganese spins J_{MnMn} independent of the Mn concentration as $J_{\mathrm{MnMn}}=Aa/2S^2$ where $a=(2/x_{eff}N_0)^{1/3}$ is the spin lattice parameter.[24] Figure 4 represents J_{MnMn} as a function of P concentration. The J_{MnMn} values are shown for $T/T_C \approx 0.4$, which is the lowest temperature for which data are available for all samples. J_{MnMn} does not scale like T_C, which points to the importance of distant Mn interaction via the hole gas.[25]

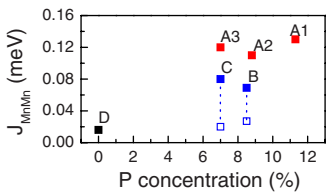

FIG. 4. (Color online) Effective exchange energy between the Mn spins J_{MnMn} as a function of P concentration at $T/T_C \approx 0.4$. For samples B and C the upper and lower boundaries for J_{MnMn} are shown by filled and open symbols, respectively.

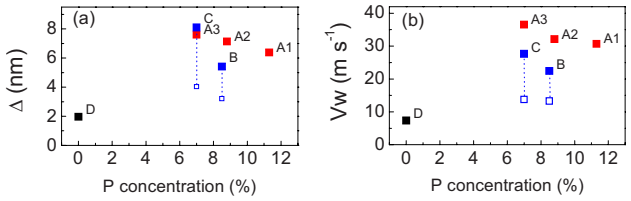

FIG. 5. (Color online) (a) DW width parameter Δ and (b) Walker velocity for DW propagation as a function of P concentration at $T/T_C \approx 0.4$. For samples B and C the upper and lower boundaries for these values are shown by filled and open symbols, respectively.

J_{MnMn} is larger for the P incorporated samples than for the (Ga,Mn)As sample by a factor up to 8. This increase might originate from an increase in the hole density n_h (sublinear dependence on n_h expected) and/or an increase in the Mn-hole exchange integral J_{pd}.[1] However, the carrier density estimated as $n_h = N_0(3x_{eff} - x_{total})/2$ (i.e., assuming interstitial Mn are the only charge compensating defects) varies only in a narrow range between 4.8×10^{20} (sample D) and 6×10^{20} cm^{-3}. These results suggest a possible increase of J_{pd} with phosphorus incorporation. A quantitative estimation of J_{pd} is however not possible without the precise determination of the carrier concentration and a theoretical description of the hole density of states in the $(\mathrm{Ga,Mn})\mathrm{As}_{1-y}\mathrm{P}_y$ alloys, which is beyond the scope of this paper.

Figure 5(a) shows the DW width parameter Δ as a function of P concentration. Δ is larger in P incorporated samples. This suggests that the DW mobility (field derivative of the DW velocity) in the field-driven DW propagation regimes, which scales like Δ, should be larger in the P-incorporated samples. We then obtain the Walker velocity $v_W = \gamma \Delta \mu_0 M_s/2$. We predict an increase in Walker velocity for the P-incorporated samples, as shown in Fig. 5(b). DW propagation experiments are needed to confirm these predictions.

As a conclusion, the novel ferromagnetic semiconductor (Ga,Mn)AsP is a very promising material for achieving FM layers with perpendicular easy axis. We have shown that the determination of the exchange constant and DW width parameter from domain theory is made more reliable than in (Ga,Mn)As owing to the self-organization of magnetic domains. This is made possible by the low density of DW pinning centers.

From the exchange constant A an effective interaction constant between Mn spins J_{MnMn} has been obtained. $(\mathrm{Ga,Mn})\mathrm{As}_{1-y}\mathrm{P}_y$ samples have a larger J_{MnMn} than the (Ga,Mn)As/GaInAs sample, however no significant enhancement of J_{MnMn} as a function of P concentration is found in the range investigated here. The Curie temperature and the ratio $[\mathrm{Mn}_{eff}]/[\mathrm{Mn}_{total}]$ do not exhibit any remarkable improvement.

The DW width parameter Δ as well as the predicted DW Walker velocity show a significant increase in the P-incorporated samples. This should be of great importance for the study of field-driven and current-driven DW propagation.

This work was in parts supported by Région Ile de France under Contract No. IF07-800/R with C'Nano IdF.

*gourdon@insp.jussieu.fr

[1] T. Jungwirth, J. Sinova, J. Mašek, J. Kučera, and A. H. MacDonald, Rev. Mod. Phys. **78**, 809 (2006).
[2] D. D. Awschalom and M. E. Flatte, Nat. Phys. **3**, 153 (2007).
[3] G. V. Astakhov, A. V. Kimel, G. M. Schott, A. A. Tsvetkov, A. Kirilyuk, D. R. Yakovlev, G. Karczewski, W. Ossau, G. Schmidt, L. W. Molenkamp, and T. Rasing, Appl. Phys. Lett. **86**, 152506 (2005).
[4] H. Munekata, Physica E (Amsterdam) **29**, 475 (2005).
[5] H. X. Tang, R. K. Kawakami, D. D. Awschalom, and M. L. Roukes, Phys. Rev. B **74**, 041310 (2006).
[6] M. Yamanouchi, D. Chiba, F. Matsukura, T. Dietl, and H. Ohno, Phys. Rev. Lett. **96**, 096601 (2006).
[7] A. Dourlat, V. Jeudy, A. Lemaître, and C. Gourdon, Phys. Rev. B **78**, 161303 (2008).
[8] J.-P. Adam, N. Vernier, J. Ferré, A. Thiaville, V. Jeudy, A. Lemaître, L. Thevenard, and G. Faini, Phys. Rev. B **80**, 193204 (2009).
[9] T. Dietl, H. Ohno, and F. Matsukura, Phys. Rev. B **63**, 195205 (2001).
[10] L. Thevenard, L. Largeau, O. Mauguin, G. Patriarche, A. Lemaître, N. Vernier, and J. Ferré, Phys. Rev. B **73**, 195331 (2006).
[11] A. Dourlat, V. Jeudy, C. Testelin, F. Bernardot, K. Khazen, C. Gourdon, L. Thevenard, L. Largeau, O. Mauguin, and A. Lemaître, J. Appl. Phys. **102**, 023913 (2007).
[12] M. Cubukcu, H. J. von Bardeleben, K. Khazen, J. L. Cantin, O. Mauguin, L. Largeau, and A. Lemaître, Phys. Rev. B **81**, 041202 (2010).
[13] A. Lemaître, A. Miard, L. Travers, O. Mauguin, L. Largeau, C. Gourdon, V. Jeudy, M. Tran, and J.-M. George, Appl. Phys. Lett. **93**, 021123 (2008).
[14] J. Mašek, J. Kudrnovský, F. Máca, J. Sinova, A. H. MacDonald, R. P. Campion, B. L. Gallagher, and T. Jungwirth, Phys. Rev. B **75**, 045202 (2007).
[15] J. C. Slonczewski, J. Appl. Phys. **45**, 2705 (1974).
[16] A. Hubert and R. Schäfer, *Magnetic Domains* (Springer, New York, 2000).
[17] T. Dietl, J. König, and A. H. MacDonald, Phys. Rev. B **64**, 241201 (2001).
[18] G. Vértesy and I. Tomáš, J. Appl. Phys. **93**, 4040 (2003).
[19] C. Gourdon, A. Dourlat, V. Jeudy, K. Khazen, H. J. von Bardeleben, L. Thevenard, and A. Lemaître, Phys. Rev. B **76**, 241301 (2007).
[20] J. Smit and H. J. Beljers, Philips Res. Rep. **10**, 113 (1955).
[21] The OOMMF code is available at http://math.nist.gov/oommf
[22] A. Hubert, J. Appl. Phys. **46**, 2276 (1975).
[23] C. Kittel, Rev. Mod. Phys. **21**, 541 (1949).
[24] Note that the underestimated average Mn-Mn distance used in Ref. 12 and also in S. T. B. Goennenwein *et al.*, Appl. Phys. Lett. **82**, 730 (2003) results in a J_{MnMn} value larger than ours by a factor $(8\pi/3)^{2/3} \approx 4$.
[25] R. Bouzerar, G. Bouzerar, and T. Ziman, EPL **78**, 67003 (2007).